

# Registration Methods for Thermal Images of Diabetic Foot Monitoring: A Comparative Study

Doha Bouallal<sup>1\*</sup>, Hassan Douzi<sup>2</sup>, Rachid Harba<sup>3</sup>  
IRF-SIC Laboratory, Ibn Zohr University, Agadir, Morocco<sup>1,2</sup>  
PRISME Laboratory, Orléans University, Orléans, France<sup>1,2,3</sup>

**Abstract**—This paper presents a comparative study of image registration techniques for Diabetic Foot (DF) thermal images. Four registration methods (Intensity-based algorithm, Iterative closest point (ICP), subpixel registration algorithm, which is mainly based on Fast Fourier Transform (FFT), and the pyramid approach for subpixel registration) have been implemented and analyzed. The performances of the four algorithms were evaluated using several overlap and symmetry metrics such as the Dice similarity coefficient (DSC), Root Mean Square Error (RMSE) and peak signal to noise ratio (PSNR). The methods were analyzed in a first step on the images of contralateral feet (right and left) of the same subject, which is called in this paper "contralateral registration" and in a second step on a pair of images of the same subject but acquired in two different times T0 and T10 after applying a cold stress test, which is called "multitemporal registration". Results showed that the intensity-based approach and the pyramid approach for subpixel registration algorithm give the best results in both types of registration (contralateral / multitemporal) and can be used efficiently for the registration of these types of images even under changing conditions.

**Keywords**—Medical imaging; diabetic foot; thermography; registration; mobile health

## I. INTRODUCTION

According to the World Health Organization (WHO) [1], by 2030 diabetes will be ranked the 7th leading cause of death worldwide. Type II diabetes (formerly known as non-insulin dependent diabetes or mature diabetes) results from a misuse of insulin by the body. It represents the majority of diabetes cases. It is largely the result of being overweight and not being physically active. A poorly controlled diabetes has a damaging impact on several organs of the body, namely the eyes (blindness), the kidneys (nephropathy) or renal failure, the heart (cardiac accident), the nervous system (neuropathy), the blood vessels (ischemia, stroke) and complications in the feet as ulcers that can lead to amputation of the lower limbs, known by the diabetic foot (DF) [2] which represents the core of our study. Diabetic foot ulcers are invariably preceded by inflammation, the presence of infection and pain. However, in the early stages of wound development, patients with diabetes may have difficulty experiencing pain due to neuropathic sensory loss [3]. On the other hand, inflammation can be identified by assessing the temperature of the affected foot. Thus, temperature assessment using a thermal camera appears to be a useful predictor of foot ulceration. Research shows that there is a significant relationship between increased temperature and diabetic foot complications [4][5].

Increased temperature can be detected up to a week before foot ulceration occurs. The most commonly used criterion is that if the point to point temperature difference  $\Delta T$  of the corresponding area of the right and left foot is greater than  $2.2^{\circ}\text{C}$  [6], there is a high risk of infection or ulceration in diabetic feet. This is called hyperthermia (see Fig. 1) and this temperature difference map is calculated point-to-point between the left and right foot after the process of registration and overlap.

Thermography is a non-invasive technology and does not require any contact with the patient's skin. This allows using it to avoid any undesirable pressures that could affect the temperature measurement, as well as the transmission of pathological organisms. For all these reasons, it has been adopted as the main technology in our study.

In the literature, there are similar works for detecting hyperthermia areas in DF. Fraiwan et al. [7], used intensity-based registration after segmenting the two plantar surfaces using Histogram shape thresholding, to align the two feet and detect the hyperthermia areas. In [8] they used ICP to register the two feet and calculate the point-to-point temperature difference.

Except that in these works the authors did not detail the performance of these methods or provide quantitative evaluations to assess the accuracy of the registration.

Kaabouch et al [9] separated the original image into two (left foot, right foot), identified the centroid and the farthest heel points of each foot, in order to calculate the angle of the feature line with respect to the vertical direction, finally they apply translation and rotation to adjust both feet in the center of the image and this technique is limited because it assumes that both feet are on the same plane in the image and have the same shape and size.

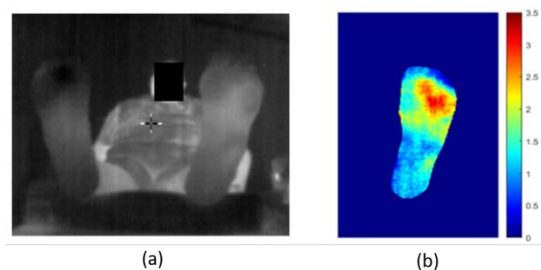


Fig. 1. Original Thermal Image, (b) Thermal difference Map  $|\Delta T|$  for a Subject with an Ulcer.

\*Corresponding Author.

In this paper, we analyze four different registration methods to obtain foot images aligned with high accuracy, in order to perform the thermal monitoring analysis, namely, the calculation of  $|\Delta T|$  between the contralateral feet as shown in Fig. 1. This registration step requires high precision, because any deviation between the feet images will have a direct impact on the accuracy of detecting abnormal plantar temperature.

The rest of the paper is organized as follows. Section 2 called materials and methods describes the acquisition protocol of our data, the used equipment, and subjects who participated to our acquisition campaign. It presents also the existing thermal analysis for DF assessment, as well as the compared registration techniques. The third section is dedicated to the quantitative and qualitative results of the tested methods. Finally, the conclusion is presented in the last section.

## II. MATERIALS AND METHODS

### A. Image Acquisition

In this section, we first explain the choice of the smartphone thermal camera, then, we describe the acquisition protocol of our images and the recruitment of participants.

1) *The chosen camera:* is the FlirOne Pro camera, designed to be connected to a smartphone. This camera consists of two sensors. A thermal sensor that measures heat through infrared emission, and an RGB sensor designed to acquire visible images in parallel with the thermal core. The camera has a thermal image resolution of 160x120 pixels and a spectral range of 8-14  $\mu\text{m}$ . FlirOne Pro can detect temperature differences of 0.1°C, which is sufficient to detect possible hyperthermia variations. It was used with a smartphone Samsung Galaxy S8.

2) *Acquisition protocol:* To collect our images, we adopted two acquisition protocols, the first one allows to obtain a single thermal image of the patient's feet, after letting him rest for 15 min (Fig. 2). The second one called Cold Stress test [10] is a protocol that consists in taking two acquisitions of the same patient in two different moments (Fig. 3).

As shown in Fig. 2, after the medical examination, Patients are requested to rest barefoot for a 15 minutes interval to allow the feet to regain their normal temperature. Finally, thermal and RGB images are acquired.

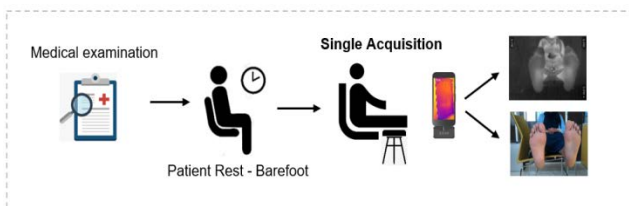


Fig. 2. Acquisition Protocol (Single Acquisition).

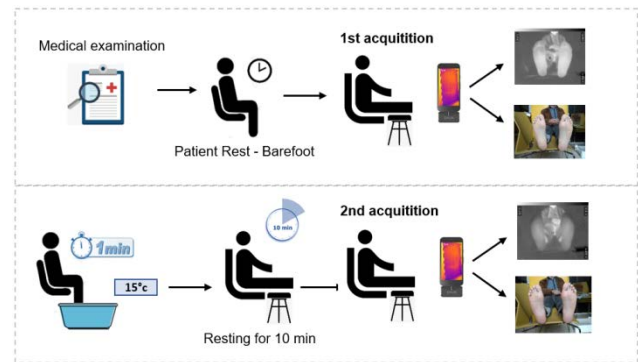


Fig. 3. Cold Stress Test Protocol (Multitemporal Acquisition).

Participants are asked to remove their shoes and socks. After a 15 minutes interval to allow the feet to recover their normal temperature, the person laid down on a stretcher or chair and placed his/her feet at the end of the stretcher, in a vertical position, and 10 cm apart. The baseline thermal image was taken freehandedly using a Samsung Galaxy S8 and a FLIR ONE Pro camera. After that, the patient is asked to immerse the feet, which are protected with thin plastic for 60 seconds in water at 15°C. After 10 minutes, a new plantar thermal image is recorded. Fig. 3 illustrates the protocol step by step.

### 3) Subjects:

a) *Control group:* Composed of 82 healthy (non-diabetic) individuals who participated in two acquisition campaigns. The first one was conducted at the University of Orleans, France. Participants were members of Prisme staff. A total of 22 people participated in this first acquisition campaign. The second acquisition campaign was organized at the IBN Zohr University in Agadir, Morocco. In which volunteer students and members of the IRF-SIC laboratory without a history of diabetes participated. In this campaign, two acquisitions were carried out for 43 people in two different moments applying the protocol of the cold stress test described in Fig. 3. In addition to 17 people who participated in a single acquisition (Fig. 2). The criteria for recruiting individuals were simple: any adult volunteer who is non-diabetic and does not have a foot problem.

b) *Diabetic group:* 145 diabetic persons accepted to participate to our study within the diabetic Foot Service of the national hospital Dos De Mayo de Lima in Perou, and signed the informed consent form. For this campaign, we exclude patients with ulcers, partial or total amputations. All acquisitions and tests were carried out under the supervision of specialists and diabetologists, who performed a set of clinical examinations on the patients to monitor neuropathy and ischemia. Two images were captured for each patient at two different moments after applying the cold stress test (Fig. 3).

## B. DF Thermal Analysis Methods

The analyses of diabetic foot thermograms can be divided into three main categories, according to existing works in the literature. The first is the asymmetric analysis between the two feet of the patient. As several studies have shown [11][3][6], there is contralateral symmetry in the distribution of skin temperature in healthy individuals, and any asymmetry in this distribution may be indicative of an abnormality. Therefore, many scientific experiments are conducted on diabetic patients [4][8][12][13][14][10][15][16] in which they found that a temperature variation of  $2.2^{\circ}\text{C}$  or more between the two feet (right and left) was detected in diabetic patients who are at risk of developing ulcers in these hyperthermic areas (see Fig. 1). The second type of thermal analysis is temperature distribution analysis [17]. The advantage of this type of analysis is that the temperature difference between the contralateral feet is no longer used and each foot can be analyzed separately. In the majority of the works based on this type of analysis, they divide the feet into several regions called angiosomes [18] by which they classify the patient's foot as being at risk of ulceration [19] [20]. The last type of analysis is based on external stress; the purpose of this analysis is to observe the response of the body thermoregulation system after applying a specific stress. This stress can vary from immersing limb in hot or cold water [10] [21], or it can be a mechanical stress such as walking or running [22]. This evaluation was presented in [21] by the thermal recovery index (TRI) which is calculated between the feet of the same patient in two different moments before and after stress). As in the study [10], they evaluated the relationship between plantar foot temperature variation and cold stress test applied on diabetic patients, by calculating the difference in temperature of the same foot at two different times, which is called a multitemporal analysis.

These thermal analyses require a series of pre-processing steps of the foot thermograms, to prepare these zones of interest which are the plantar soles. The first task consists in segmenting the two feet and separating them from the rest of the background (Fig. 4), and in this study the images we are going to present are previously segmented using a neural architecture that is detailed in our previous work [23].

Once the feet have been segmented, a primordial step is to align the feet in order to calculate the temperature difference either by applying the contralateral analysis (asymmetry) or the analysis based on the external stress (multitemporal). This step is the core of this work. Our objective is to find the most suitable registration method for our problem, which can be defined by two essential challenges;

- Variation in shape and position between the patient's feet, which complicates the registration.
- Dissimilarity between two images of the same patient foot taken at different times (in our case instant  $T_0$  before cold stress test and instant  $T_{10}$  after cold stress test), from different distances, or from different viewpoints.

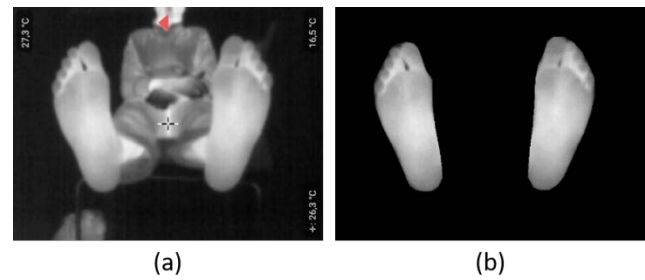


Fig. 4. (a) Thermal Image, (b) Segmented Feet.

## C. Image Registration

1) *Registration types*: In this work we conducted two types of experiments. The first one is a contralateral registration, which consists of aligning the right and left feet of the same patient image. And the second is a multitemporal registration applied on a pair of images of the same feet acquired in two different moments with the cold stress test.

a) *Contralateral registration*: the first dataset consists of thermal images of segmented feet as shown in Fig. 4(b). The image of the two feet is divided into two (left foot and right foot), the right foot is considered as the reference image (fixed) and the left foot (moving) is flipped horizontally to register it with the reference image, in order to calculate the temperature difference between the two feet after aligning them. The process is detailed in Fig. 5.

b) *Multitemporal registration*: this type consists of registering a pair of thermal images of the same patient taken at two different times. A first acquisition at time  $T_0$  captured before the application of the cold stress test [10] and a second acquisition at time  $T_{10}$  made 10 min after the application of the cold stress test.

This is a multitemporal registration in which the goal is to align the two images of the same foot at two different times  $T_0$  and  $T_{10}$ . The image of the right foot at time  $T_{10}$ , which is considered as a target (moving image), is aligned with the image of the right foot at  $T_0$ , which is considered as a reference image (fixed image), and the same for the left foot. The process is shown in Fig. 6.

2) *Registration techniques*: In our research, the objective is not to make the foot images identical. We are looking for the transformation that minimizes the distance between the information contained in one image and its correspondence on the other image. As well as studying the significant differences that will allow us to localize the region at risk of ulceration. In our case, the registration must not modify the size of potential anomalies, or make local deformations on the foot, since this could, for example, mask the detection of a hyperthermia area. Therefore, the registration methods chosen in this paper are linear, either rigid transformations (translation-rotation) such as the ICP [24] and the Sicairos et al. method [25], or affine transformations, namely intensity-based algorithm [26] and pyramid approach [27]. In the following, we will present the registration techniques that we have compared and evaluated on our database.

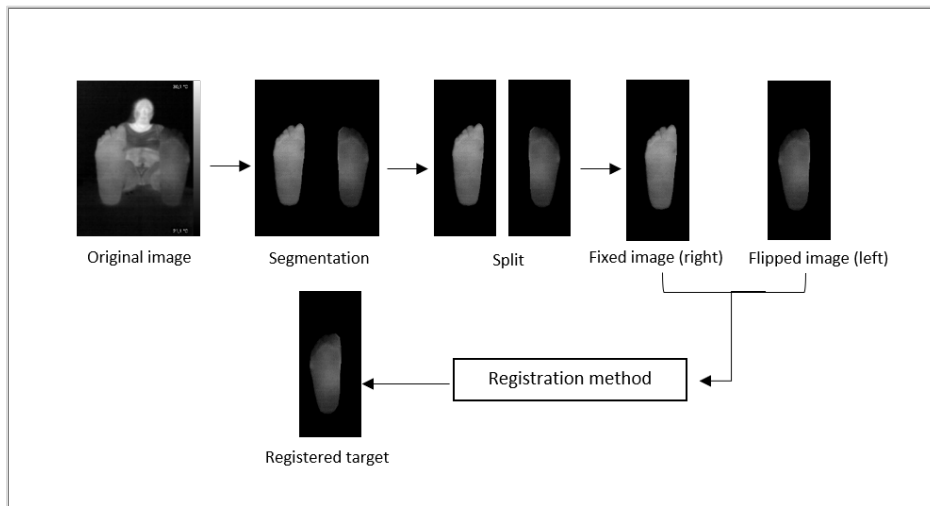


Fig. 5. Contralateral Registration Process.

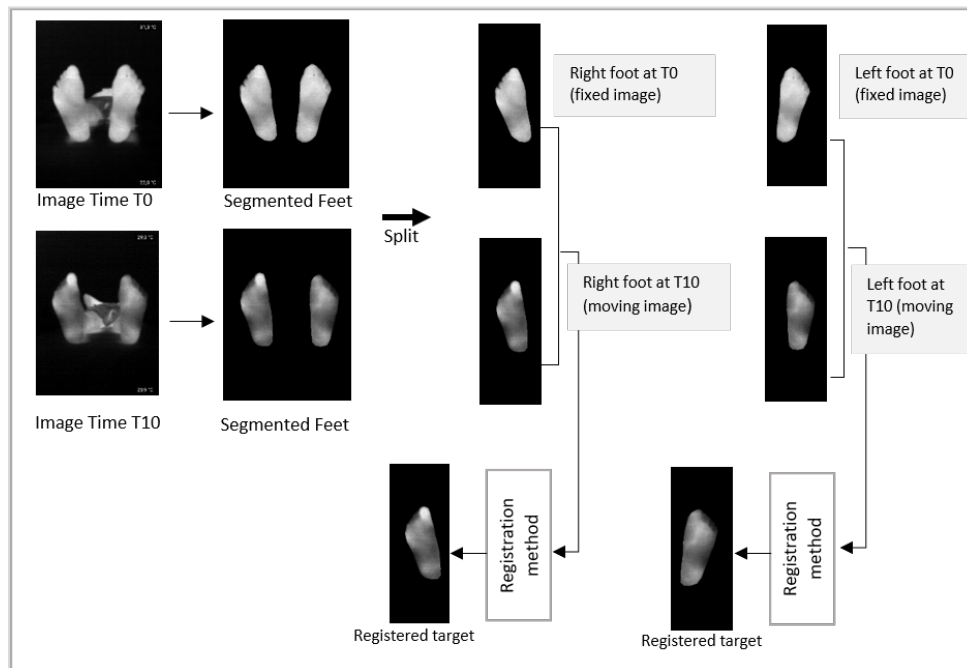


Fig. 6. Multitemporal Registration (after Applying Cold Stress Test).

a) *Iterative Closest Point (ICP)*: The Iterative Closest Point (ICP) algorithm is used to match two sets of data, most often in the form of point clouds or meshes corresponding to two partial views of the same object. Iteratively, the algorithm revises the transformation (combination of translation and rotation) needed to minimize an error metric, usually a distance between the source and target point clouds, such as the sum of squared differences between the coordinates of the matched pairs.

In this work, we used a maximum number of iterations of 300 and a minimum difference in the correspondence measure between two successive iterations of  $1e^{-5}$ . These values were chosen empirically, after a number of tests, as it was observed that no more than 300 iterations were required in any of the studied cases to converge to an optimal solution.

b) *Sicairos et al approach*: To perform a simple translation between two images, the usual technique for solving this problem is to compute an oversampled cross-correlation between the image to be registered and a reference image, using a Fast Fourier Transform (FFT), and locate its peak. The computational burden associated with this approach increases as the accuracy required for the registration increases, especially in terms of memory.

Therefore, as an alternative Guizar-Sicairos et al. [25] have developed different algorithms that significantly improve performance without sacrificing accuracy. These algorithms start with an initial estimation of the location of the cross-correlation peak obtained by the FFT method with an upsampling factor of  $k_0=2$ . This initial upsampling is used for the purpose of selecting an appropriate starting point for cross-

correlations that might have more than one peak of similar magnitude. This type of algorithm, as in the FFT upsampling approach, always uses all the information available in the images to compute the initial estimate and each point of the upsampled cross-correlation grid, which makes it very robust to noise. It has been demonstrated in [25] that these new registration refinement algorithms can achieve subpixel image registration with the same or better accuracy than traditional FFT oversampling but with significantly reduced computation time and memory requirements.

c) *Intensity-based registration:* The intensity-based registration method operates directly on the gray values of the images. The main goal of this technique is to find the right transformation that maximizes (or minimizes) the similarity metric between the corresponding voxels.

The most frequently used similarity measures are the sum of squared differences of pixel intensities, the regional correction or the mutual information.

As shown in the Fig. 7, the algorithm takes two images in input, the image to be registered (moving image) and the reference image (fixed image). It requires four other essential parameters, namely; a similarity metric, an optimizer and the type of transformation.

The process begins with the transformation type we specify and an internally determined transformation matrix. They jointly determine the specific image transformation which is applied to the moving image with a bilinear interpolation. Then the metric compares the transformed moving image to the fixed image and a metric value is returned.

Finally, the process stops when it has reached a point of decreasing efficiency or has reached the maximum number of iterations. If there is no stopping condition, the optimizer adjusts the transformation to start the next iteration.

In this experiment, we ran the intensity-based algorithm using One Plus One Evolutionary optimizer with an initial radius of  $6,25 e^{-3}/3,5$ , growth factor of 1,05 and a maximum iterations number of 300. The similarity metric used is a mattes mutual information metric. For the initial transformation type, we used affine transformation. These chosen parameters are the ones that gave the best results after several tests.

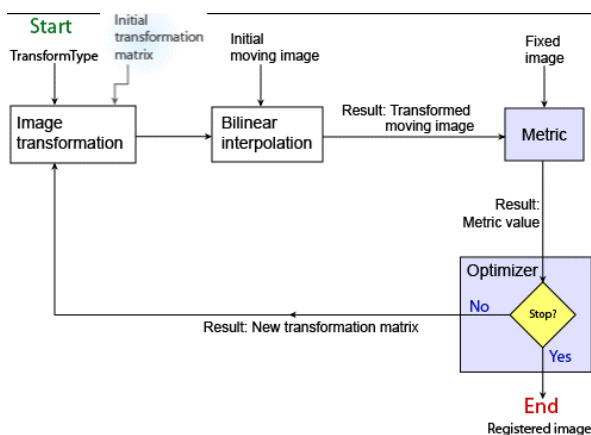


Fig. 7. Intensity-based Registration Algorithm [23].

d) *Pyramid Approach for subpixel registration:* Thévenaz et al. [27] proposed an automatic sub-pixel registration algorithm that minimizes the mean square intensity difference between a reference data set and a test data set, which can be images (two-dimensional) or even volumes (three-dimensional). This method uses an explicit spline representation of the images in conjunction with spline processing, and is based on a coarse-to-fine iterative strategy (pyramid approach).

The minimization is performed according to a new variation (ML\*) of the Marquardt-Levenberg algorithm [28] for nonlinear least squares optimization. The geometric deformation model consists of a global three-dimensional (3D) affine transformation that can optionally be restricted to rigid body motion (rotation and translation), combined with isometric scaling. It also includes an optional adjustment of the contrast differences of the images.

According to [27], this algorithm has shown excellent results for the registration of intramodal positron emission tomography (PET) and functional magnetic resonance imaging (fMRI) data.

### III. RESULTS

In order to assess the best approach for registering the thermal infrared images of the diabetic foot application, we have tested the four registration methods on our two types of acquisitions, the first “Contralateral” (Fig. 5) containing one image of the feet of each patient (left, right) and the second “Multitemporal” (Fig. 6) containing a pair of images of the same feet acquired at two different times. The purpose is to evaluate the robustness of these approaches in both cases of registration (contralateral/multitemporal) and under the changes that can occur in the position of the subject’s feet, changes in the distance of acquisition or viewpoints, especially for the images captured at two different times.

#### A. Evaluation Metrics

To quantitatively evaluate the performance of these algorithms, we adopted three evaluation metrics that are most commonly used in the field of registration evaluation. The first one is the Dice similarity Coefficient (DSC) [20], the second one is the RMSE (Root Mean square error) and the last one is PSNR (Peak Signal to Noise Ratio).

- Dice similarity coefficient (DSC): is a statistical indicator that measures the similarity of two samples.
- This score quantifies the overlap between the fixed foot and the registered one.

$$DSC = \frac{2 * |X \cap Y|}{|X| + |Y|} \quad (1)$$

X is the reference image and Y is the registered image.

- Root Mean Square error (RMSE): used to measure the difference per pixel between the moving image and reference image. The lower the value of RMSE, the better the registration performance.

$$RMSE(X, Y) = \sqrt{\frac{\sum_{i=1}^n (X_i - Y_i)^2}{n}} \quad (2)$$

where, X and Y are respectively the reference image and the registered image. n is the total number of pixels in the image.

- Peak Signal to noise ratio (PSNR) : is identified as a numerical measure for image registration quality based on the pixel differences between two images [29]. The Mathematical equation is provided as in equation 3 based on [29]. Where  $MAX_I$  is the maximum possible pixel value of the image and MSE is mean square error between reference and target image. A higher PSNR value indicates a higher similarity between registered images. Contrarily, the smaller PSNR value indicates poor similarity between images.

$$PSNR = 10 \cdot \log_{10} \left( \frac{MAX_I^2}{MSE} \right) \quad (3)$$

$$MSE = \frac{1}{n} \sum_{i=1}^n (Xi - Yi)^2 \quad (4)$$

### B. Comparative Results

From the results in Tables I and II, on one hand we deduce that the intensity-based method gives the best value for the Dice coefficient (0.97) followed by the pyramid method (0.96). (The best results are highlighted in bold). On the other hand, we notice that the four algorithms are more robust in the first type of registration (contralateral registration), which is reasonable, since in these acquisitions the two feet to be registered (right and left) are positioned at the same distance from the camera. So generally, in this case we are in front of geometrical transformations that can be considered as a combination of translation and rotation.

TABLE I. COMPARATIVE RESULTS FOR CONTRALATERAL REGISTRATION BETWEEN RIGHT AND LEFT FEET

Methods \ Metrics	Intensity based registration	ICP	Sicairos et al	Pyramid approach
DSC	<b>0,97</b>	0,95	0,93	0,96
RMSE	0,245	0,315	0,34	<b>0,23</b>
PSNR	25,85	23,62	22,90	<b>26,41</b>

TABLE II. COMPARATIVE RESULTS FOR MULTITEMPORAL REGISTRATION

Methods \ Metrics	Intensity based registration	ICP	Sicairos et al	Pyramid approach
DSC	<b>0,968</b>	0,905	0,89	0,94
RMSE	0,344	0,445	0,442	<b>0,318</b>
PSNR	22,24	19,85	19,85	<b>23</b>

Contrary to multi-temporal registration, in which we can clearly see that in some cases, the acquirer can change the distance and position of the camera between time T0 and T10 (ex: Fig. 12). With smartphone, freehandedly, the distance between the feet and the camera may slightly change. This generates a change of scale between the two feet, making the task of registration more complicated.

Based on the results of the two previous tables (Tables I and II) and the charts in the two Fig. 8, 9 and 10, we can see that the performance of the compared methods has decreased

between the contralateral and the multitemporal registration. For example, in Fig. 9 we have the ICP method with a DSC of 0.95 as a result of final overlap of the registered feet (right and left), this value decreased to 0.90 when applying ICP on the images of the same feet acquired at two different times, a difference of 5%.

And this is expected, since the transformation applied by ICP cannot perform perspective corrections. While in the images of the cold stress test the person making the acquisitions often changes the distance and position of the camera between the two instants. The only method that kept the same performance between the two types of registration is the intensity-based method. As shown in Fig. 9 dice values for multitemporal and contralateral registration are almost identical for this method, unlike the other algorithms.

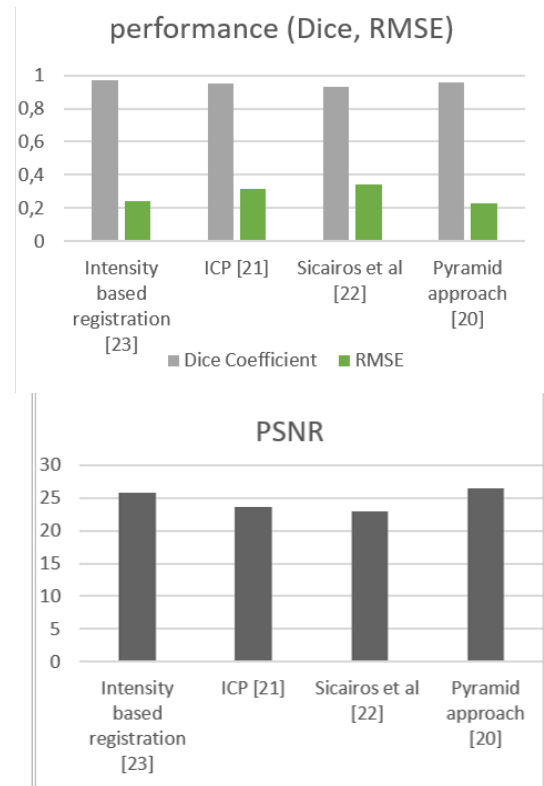


Fig. 8. Dice Coefficient, RMSE and PSNR Metrics for the Four Registration Methods Obtained with Images of Contralateral Feet (Registration between Right and Left Foot).

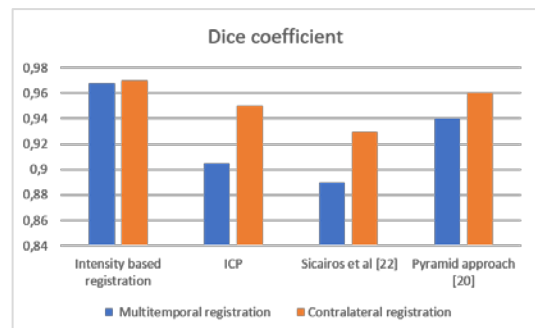


Fig. 9. Dice Coefficient of the Four Registration Methods to Evaluate their Performance in Both Type of Registration (Contralateral and Multitemporal).

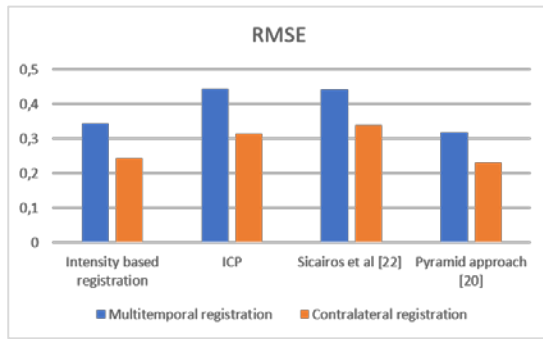


Fig. 10. RMSE of the Four Registration Methods to Evaluate their Performance in Both Type of Registration (Contralateral and Multitemporal).

The qualitative results are in total agreement with the results calculated above (Tables I and II), we see that in Fig. 11 All four registration methods obtain a visually correct overlap between the fixed thermal image and the registered foot when both feet of the subject are located at the same distance from the camera. And the two algorithms based on the intensity and the one of Th evenaz et al [27] (pyramid registration approach) give the best performances.

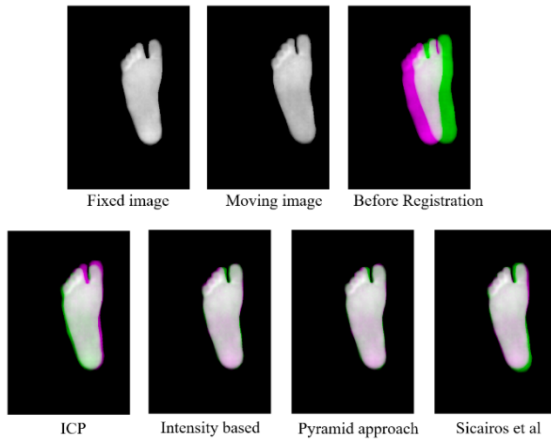


Fig. 11. Example of Contralateral Registration (Left Foot and Right Foot). in All Images, the Foot in Pink is the Fixed Foot (Right) and the Foot in Green is the Moving Foot (Left).

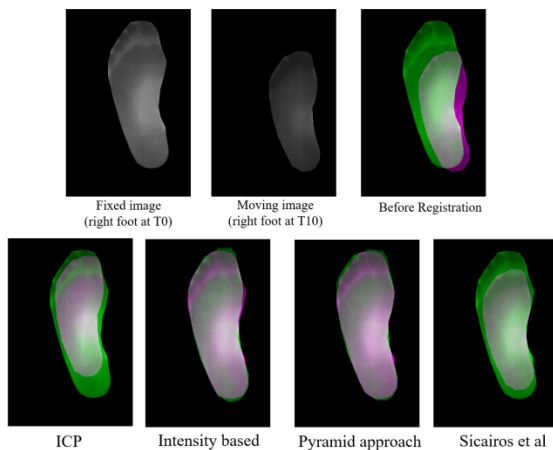


Fig. 12. Example of Multitemporal Registration (Right Foot at Time T0 and Right Foot at Time T10). in All Images, the Foot in Green is the Fixed Foot (Right Foot T0) and the Foot in Pink is the Moving Foot (Right Foot T10).

For multitemporal registration, as shown in Fig. 12 and 13, the added challenges to the algorithms are the change of the capturing view point and the difference distance from the camera between the acquisition at time T0 and the second acquisition at time T10. The methods that have proven their robustness in these cases are intensity based and pyramid approach. They align the images, where the feet don't have the same size and shape. Unlike the method of [9] which is limited and only works in the case where both feet are on the same plane in the image and have the same shape and size.

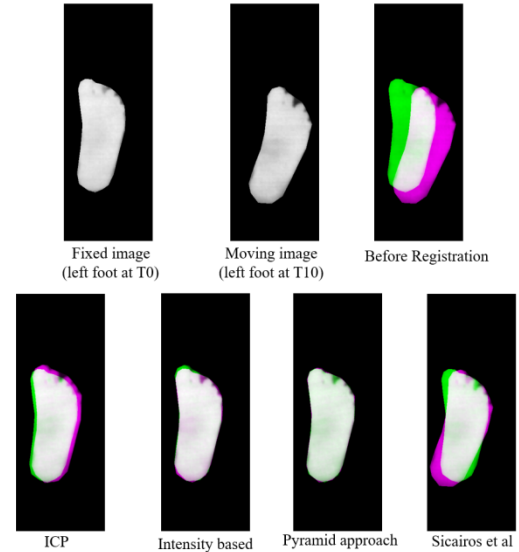


Fig. 13. Example of Multitemporal Registration (Left Foot at Time T0 and Left Foot at Time T10). in All Images, the Foot in Green is the Fixed Foot (Left Foot T0) and the Foot in Pink is the Moving Foot (Left Foot T10).

#### IV. CONCLUSION

To diagnose the DF problem at an early stage and to detect the areas at risk of ulceration, it is necessary to have a fast and non-contact procedure with simple and low-cost devices. In order to achieve this goal, it is important to implement an approach with a high-level accuracy in diagnosis, ensuring that the acquisition and processing of data does not introduce systematic errors that can be avoided at the time of conception.

Medical diagnostic devices of DF supposed to perform these thermal analyses; such as the computation of temperature difference between contralateral feet or between feet after application of external stresses, require a correct alignment of the acquired images. Because any deviation between the images of the feet will have a direct impact on the accuracy of the subsequent abnormal temperature detection. Hence, the need to evaluate the performance of the registration techniques is used at the heart of this alignment.

In this work, a group of registration methods was implemented and evaluated to match thermal images for diabetic foot application. For the registration of contralateral feet, the methods compared in this paper gave satisfying results. However, when applying the multitemporal registration which consists in aligning the same foot captured in two different instants (T0 and T10), we notice that the performances of ICP and Sicairos et al method have decreased.

This can be explained by the complexity increased by changing the capturing view point and distance in two different moments.

While Intensity-based algorithm and pyramid approach have proved their stability and robustness in both types of registration, especially the intensity-based method, this is confirmed by the Dice coefficients obtained, which are 0.97 and 0.96 for intensity and pyramid respectively, in the case of contralateral registration. 0.968 and 0.94 in the case of multitemporal registration regardless of the distance between the subject and the camera.

This comparative study permitted to find the registration method that fits the most to our thermal images, with all their specificities and their complexity related to the adopted acquisition protocol. This "free hand" protocol is based mainly on a smartphone and the dedicated thermal camera. Even if on one hand it complicates the tasks of image processing such as segmentation and registration, on the other hand, it allows using the diagnosis system by patient in a convivial and simple way, without needing the intervention of a specialist.

In the future, we intend to develop thermal analysis approaches for the detection of hyperthermia areas. Subsequently we envisage combining and improving all these techniques, in order to integrate them into a complete system of diagnostic to help doctors and podiatrists to identify DF disorders in early stages. This will certainly decrease the risks of ulcerations and amputations.

#### ACKNOWLEDGMENT

This work was supported by the European Union's project Standup Horizon 2020 #777661. A research and innovation program under the Marie Skłodowska-Curie. Aiming to develop smartphone applications for prevention and supervision of diabetic foot ulcers. We thank all our participants for their contributions.

#### REFERENCES

[1] « Diabète ». <https://www.who.int/fr/news-room/factsheets/detail/diabetes> (consulté le 11 janvier 2022).

[2] J. J. van Netten et al., « Definitions and criteria for diabetic foot disease », *Diabetes Metab. Res. Rev.*, vol. 36, no S1, p. e3268, 2020, doi: 10.1002/dmrr.3268.

[3] A. W. Chan, I. A. MacFarlane, et D. R. Bowsher, « Contact Thermography of Painful Diabetic Neuropathic Foot », *Diabetes Care*, vol. 14, no 10, Art. no 10, oct. 1991, doi: 10.2337/diacare.14.10.918.

[4] D. G. Armstrong, K. Holtz-Neiderer, C. Wendel, M. J. Mohler, H. R. Kimbriel, et L. A. Lavery, « Skin Temperature Monitoring Reduces the Risk for Diabetic Foot Ulceration in High-risk Patients », *Am. J. Med.*, vol. 120, no 12, Art. no 12, déc. 2007, doi: 10.1016/j.amjmed.2007.06.028.

[5] S. Bagavathiappan et al., « Correlation between Plantar Foot Temperature and Diabetic Neuropathy: A Case Study by Using an Infrared Thermal Imaging Technique », *J. Diabetes Sci. Technol.*, vol. 4, no 6, Art. no 6, nov. 2010, doi: 10.1177/193229681000400613.

[6] D. Hernandez-Contreras, H. Peregrina-Barreto, J. Rangel-Magdaleno, et J. Gonzalez-Bernal, « Narrative review: Diabetic foot and infrared thermography », *Infrared Phys. Technol.*, vol. 78, p. 105-117, sept. 2016, doi: 10.1016/j.infrared.2016.07.013.

[7] « Fraiwan et al. - 2017 - Diabetic foot ulcer mobile detection system using .pdf ».

[8] L. Vilcahuaman et al., « Automatic Analysis of Plantar Foot Thermal Images in at-Risk Type II Diabetes by Using an Infrared Camera », in

*World Congress on Medical Physics and Biomedical Engineering, June 7-12, 2015, Toronto, Canada*, vol. 51, D. A. Jaffray, Éd. Cham: Springer International Publishing, 2015, p. 228-231. doi: 10.1007/978-3-319-19387-8\_55.

[9] « Kaabouch et al. - 2009 - Asymmetry analysis based on genetic algorithms for.pdf ».

[10] D. Bouallal et al., « Segmentation of plantar foot thermal images: application to diabetic foot diagnosis », in *2020 International Conference on Systems, Signals and Image Processing (IWSSIP)*, Niterói, Brazil, juill. 2020, p. 116-121. doi: 10.1109/IWSSIP48289.2020.9145167.

[11] B. F. Jones, « A reappraisal of the use of infrared thermal image analysis in medicine », *IEEE Trans. Med. Imaging*, vol. 17, n° 6, Art. n° 6, déc. 1998, doi: 10.1109/42.746635.

[12] N. Kaabouch, Y. Chen, W.-C. Hu, J. Anderson, F. Ames, et R. Paulson, « Early detection of foot ulcers through asymmetry analysis », *Lake Buena Vista, FL*, févr. 2009, p. 72621L. doi: 10.1117/12.811676.

[13] N. Kaabouch, Y. Chen, J. Anderson, F. Ames, et R. Paulson, « Asymmetry analysis based on genetic algorithms for the prediction of foot ulcers », *San Jose, CA*, janv. 2009, p. 724304. doi: 10.1117/12.805975.

[14] N. Kaabouch, « Enhancement of the asymmetry-based overlapping analysis through features extraction », *J. Electron. Imaging*, vol. 20, n° 1, Art. n° 1, janv. 2011, doi: 10.1117/1.3553240.

[15] C. Liu, J. J. van Netten, J. G. van Baal, S. A. Bus, et F. van der Heijden, « Automatic detection of diabetic foot complications with infrared thermography by asymmetric analysis », *J. Biomed. Opt.*, vol. 20, n° 2, Art. n° 2, févr. 2015, doi: 10.1117/1.JBO.20.2.026003.

[16] J. J. van Netten, M. Prijs, J. G. van Baal, C. Liu, F. van der Heijden, et S. A. Bus, « Diagnostic values for skin temperature assessment to detect diabetes-related foot complications », *Diabetes Technol. Ther.*, vol. 16, n° 11, p. 714-721, nov. 2014, doi: 10.1089/dia.2014.0052.

[17] T. Mori et al., « Morphological Pattern Classification System for Plantar Thermography of Patients with Diabetes », *J. Diabetes Sci. Technol.*, vol. 7, n° 5, Art. n° 5, sept. 2013, doi: 10.1177/193229681300700502.

[18] C. Attinger, K. Evans, E. Bulan, P. Blume, et P. Cooper, « Angiosomes of the Foot and Ankle and Clinical Implications for Limb Salvage: Reconstruction, Incisions, and Revascularization », *Plast. Reconstr. Surg.*, vol. 117, n° 7S, Art. n° 7S, juin 2006, doi: 10.1097/01.prs.0000222582.84385.54.

[19] T. Nagase et al., « Variations of plantar thermographic patterns in normal controls and non-ulcer diabetic patients: Novel classification using angiosome concept », *J. Plast. Reconstr. Aesthet. Surg.*, vol. 64, n° 7, Art. n° 7, juill. 2011, doi: 10.1016/j.jbjs.2010.12.003.

[20] G. I. Taylor et J. H. Palmer, « The vascular territories (angiosomes) of the body: experimental study and clinical applications », *Br. J. Plast. Surg.*, vol. 40, n° 2, Art. n° 2, mars 1987.

[21] L. F. Balbinot, L. H. Canani, C. C. Robinson, M. Achaval, et M. A. Zaro, « Plantar thermography is useful in the early diagnosis of diabetic neuropathy », *Clinics*, vol. 67, n° 12, p. 1419-1425, déc. 2012, doi: 10.6061/clinics/2012(12)12.

[22] M. Yavuz et al., « Temperature as a predictive tool for plantar triaxial loading », *J. Biomech.*, vol. 47, n° 15, p. 3767-3770, nov. 2014, doi: 10.1016/j.jbiomech.2014.09.028.

[23] D. Bouallal, H. Douzi, et R. Harba, « Diabetic foot thermal image segmentation using Double Encoder-ResUnet (DE-ResUnet) », *J. Med. Eng. Technol.*, vol. 0, n° 0, p. 1-15, mai 2022, doi: 10.1080/03091902.2022.2077997.

[24] P. J. Besl et N. D. McKay, « A method for registration of 3-D shapes », *IEEE Trans. Pattern Anal. Mach. Intell.*, vol. 14, n° 2, p. 239-256, févr. 1992, doi: 10.1109/34.121791.

[25] M. Guizar-Sicairos, S. T. Thurman, et J. R. Fienup, « Efficient subpixel image registration algorithms », *Opt. Lett.*, vol. 33, n° 2, p. 156-158, janv. 2008, doi: 10.1364/OL.33.000156.

[26] « Intensity-Based Automatic Image Registration - MATLAB & Simulink ». <https://www.mathworks.com/help/images/intensity-based-automatic-image-registration.html?searchHighlight=intensity%20based%20registration&s>



- \_tid=srchtitle\_intensity%20based%20registration\_1 (consulté le 6 janvier 2022).
- [27] P. Thévenaz, U. E. Ruttimann, et M. Unser, « A pyramid approach to subpixel registration based on intensity », *IEEE Trans. Image Process. Publ. IEEE Signal Process. Soc.*, vol. 7, n° 1, p. 27-41, 1998, doi: 10.1109/83.650848.
- [28] D. W. Marquardt, « An Algorithm for Least-Squares Estimation of Nonlinear Parameters », *J. Soc. Ind. Appl. Math.*, vol. 11, n° 2, p. 431-441, 1963.
- [29] Y. Tanabe et T. Ishida, « Quantification of the accuracy limits of image registration using peak signal-to-noise ratio », *Radiol. Phys. Technol.*, vol. 10, n° 1, p. 91-94, mars 2017, doi: 10.1007/s12194-016-0372-3.